The Astronomical Journal, 153:88 (9pp), 2017 February doi:10.3847/1538-3881/153/2/88

GALACTIC EXTINCTION AND REDDENING FROM THE SOUTH GALACTIC CAP u-BAND SKY SURVEY: u-BAND GALAXY NUMBER COUNTS AND $u - r$ COLOR DISTRIBUTION

Linlin Li[1,2], Shiyin Shen[1,3], Jinliang Hou[1], Fangting Yuan[1], Jing Zhong[1], Hu Zou[4], Xu Zhou[4], Zhaoji Jiang[4], Xiyan Peng[4], Dongwei Fan[4], Xiaohui Fan[4], Zhou Fan[4], Boliang He[4], Yipeng Jing[5], Michael Lesser[6], Cheng Li[1], Jun Ma[4], Jundan Nie[4], Jiali Wang[4], Zhenyu Wu[4], Tianmeng Zhang[4], and Zhimin Zhou[4]
[1] Key Laboratory for Research in Galaxies and Cosmology, Shanghai Astronomical Observatory, Chinese Academy of Sciences, 80 Nandan Road, Shanghai, 20030, China; lilin@shao.ac.cn
[2] University of Chinese Academy of Sciences, 19A Yuquanlu, Beijing, 100049, China
[3] Key Lab for Astrophysics, Shanghai 200234, China; ssy@shao.ac.cn
[4] Key Laboratory of Optical Astronomy, National Astronomical Observatories, Chinese Academy of Sciences, Beijing, 100012, China
[5] Center for Astronomy and Astrophysics, Department of Physics and Astronomy, Shanghai Jiao Tong University, Shanghai 200240, China
[6] Steward Observatory, University of Arizona, Tucson, AZ 85721, USA
Received 2016 July 18; revised 2017 January 4; accepted 2017 January 5; published 2017 January 31

ABSTRACT

We study the integral Galactic extinction and reddening based on the galaxy catalog of the South Galactic Cap u-band Sky Survey (SCUSS), where u-band galaxy number counts and $u - r$ color distribution are used to derive the Galactic extinction and reddening respectively. We compare these independent statistical measurements with the reddening map of Schlegel et al. (SFD) and find that both the extinction and reddening from the number counts and color distribution are in good agreement with the SFD results at low extinction regions ($E(B-V)^{\rm SFD} < 0.12$ mag). However, for high extinction regions ($E(B-V)^{\rm SFD} > 0.12$ mag), the SFD map overestimates the Galactic reddening systematically, which can be approximated by a linear relation $\Delta E(B-V) = 0.43[E(B-V)^{\rm SFD} - 0.12]$. By combining the results from galaxy number counts and color distribution, we find that the shape of the Galactic extinction curve is in good agreement with the standard $R_V = 3.1$ extinction law of O'Donnell.

Key words: dust, extinction – methods: statistical – techniques: photometric

1. INTRODUCTION

Interstellar dust absorbs and scatters photons from most astronomical sources (Draine 2003), which causes extinction and reddening in observations. All extragalactic objects are extincted and reddened by the Milky Way interstellar dust (Denney et al. 2010; Oguri 2014). A map of the integral Galactic dust extinction is essential for all extragalactic studies.

The most commonly used all-sky dust extinction map was constructed by Schlegel et al. (1998) (hereafter SFD), which was derived from the composite of the COBE/DIRBE and IRAS/ISSA infrared maps and the Leiden-Dwingeloo map of HI emission. With $E(B-V)$ values provided by the SFD map, the Galactic extinction in any given photometric band can be parameterized by $A_\lambda = k(\lambda)E(B-V)$, where $k(\lambda)$ is the extinction coefficient determined by the Galactic extinction curve (see Cardelli et al. 1989 and its update by O'Donnell 1994, hereafter ODO).

The $E(B-V)$ values of the SFD map have been tested by many independent measurements. Arce & Goodman (1999) used four different methods to derive the extinction in the Taurus dark cloud complex, suggesting that the SFD map overestimates the extinction by a factor of 1.3–1.4 in regions where $A_V > 0.5$ mag (see also Dobashi et al. 2005; Schlafly et al. 2010; Schlafly & Finkbeiner 2011; Yuan et al. 2013). However, these tests are typically based on spectral types of Galactic stars. The integral line-of-sight dust to stars is not directly comparable to the integral Galactic extinction of extragalactic sources, but to its lower limit.

Galaxy number count is an independent approach that can test the integral Galactic extinction. Under the assumption of an isotropic galaxy distribution on large scales, there will be a smaller number of galaxies in the direction of higher Galactic extinction down to the same apparent magnitude (Burstein & Heiles 1982; Fukugita et al. 2004; Yasuda et al. 2007). Using the r-band galaxy number counts in the Sloan Digital Sky Survey (SDSS; York et al. 2000), Yasuda et al. (2007) found that the SFD map overestimates the Galactic extinction in high extinction regions ($E(B-V) > 0.15$ mag).

Besides the extinction effect, Galactic dust also reddens the colors of background galaxies (González et al. 1999; Schröder et al. 2007; Peek & Graves 2010). Compared with the number counts of galaxies, the average color relies less on the assumption of a homogeneous distribution of them. Using passive galaxies as color standards, Peek & Graves (2010) estimated the Galactic reddening and, in contrast, found that the SFD map under-predicts the reddening toward low Galactic latitudes (high extinction regions). However, as claimed by these authors, this result does not necessarily conflict with the galaxy number count results since the regions in this study all have $E(B-V) < 0.15$.

To have a better constraint on the Galactic extinction and resolve possible conflicts between the studies of galaxy number counts and galaxy colors, high-quality photometry data at shorter wavelength (e.g., the u band), where the extinction/reddening effect is more significant, are helpful. For the SDSS data, the photometric depth and accuracy in the u band is not comparable to the other bands due to its low efficiency. Alternatively, the South Galactic Cap u-band Sky Survey (SCUSS) (Zhou et al. 2016), which is a u-band (354 nm) survey at high latitude in the South Galactic region, and provides u-band data with a depth of about 1.5 mag deeper than with the SDSS. In this study, we take the released catalog of

SCUSS (Zou et al. 2016) to study the Galactic extinction with both the u-band galaxy number counts and $u-r$ color distribution by further combining the SDSS data. Our motivation is to take the advantages of the SCUSS u-band data and make a detailed and self-consist statistical study on the Galactic extinction and reddening in the South Galactic cap region.

This paper is organized as follows. In Section 2, we introduce the galaxy catalog related to this study. In Sections 3 and 4, we study the Galactic extinction and reddening using the u-band galaxy number counts and $u-r$ color distribution respectively. We discuss the Galactic extinction curve in Section 5. Finally, we give a brief summary in Section 6.

2. DATA

2.1. SCUSS Photometry

SCUSS is a deep (deeper than SDSS) u-band image survey in the north part of the South Galactic cap region. The effective wavelength of the SCUSS u-band filter is 3538 Å, slightly different from (bluer than) the SDSS u band. The survey is undertaken on the 2.3 m Bok telescope at Kitt Peak with a 4k × 4k CCD camera, which provides a field of view $1.^{\circ}08 \times 1.^{\circ}03$ and image resolution of 0.454 arcsec per pixel. The footprint of the survey is initially designed to be the region where $b < -30^{\circ}$ and $\delta > -10^{\circ}$ and later slightly extended to lower Galactic latitudes. Each field typically has two exposures and the total exposure time amounts to more than five minutes, which provides photometry depth of about 1.5 mag deeper than the SDSS u-band data (see further discussions in Section 2.3). The overview of the survey can be found in Zhou et al. (2016) and visited at http://batc.bao.ac.cn/Uband/. In this study, we take the released data of SCUSS, which includes 3700 fields and with a total sky coverage of about 4115 deg^2 (Zou et al. 2016). The details of the data reduction of SCUSS images can be found in Zou et al. (2015). Here, we list some key ingredients of the data reduction related to this study.

The single-epoch images are first stacked to form a combined image for each field. SExtractor (Bertin & Arnouts 1996) is then used to detect objects on the stacked images. The detected sources are named "total sources" with "automatic magnitude" recorded, and are also classified as point/extended sources according to "BERTIN_G_S." For these fields also with SDSS photometry, the "total objects" are then matched with the objects in the SDSS Data Release 9 (DR9) catalog with any of the u, g, r, i, z magnitudes measured. All the matched objects are noted as "core sources." For these "core sources," the flag "Type" in theSDSS r band replaces "BERTIN_G_S" and is used to make the star/galaxy classification. For galaxies in "core sources," their SDSS r-band de Vaucouleurs and exponential likelihoods are further adopted to derive the model magnitude ("modelMag") in the SCUSS u-band as for the "modelMag" in other SDSS bands.

In this study, we take "total sources" for u-band galaxy number counts (Section 3) and use "core sources" for reddening measurements from $u-r$ colors (Section 4). Since we aim to study the Galactic extinction using extragalactic sources, the magnitudes of all galaxies have not been corrected for Galactic extinction.

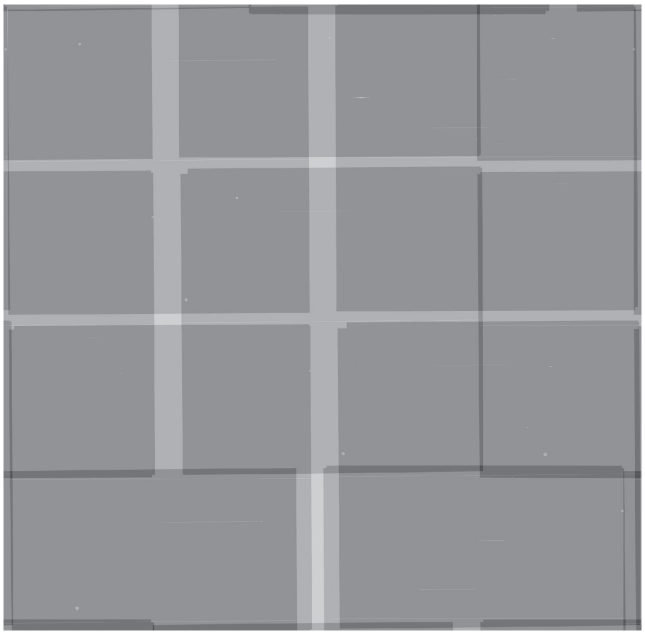

Figure 1. Exposure map of an example SCUSS field. The dark gray area (most occupied) has two exposures, while the white, gray, and black areas have 0, 1, and >2 exposures respectively.

2.2. Galaxy Sample

In this study, we take the galaxies from the region where the SCUSS overlaps with the SDSS. The SDSS footprint in the south Galactic region is about 5192 deg^2 and its photometry catalog had been released in DR8 (Aihara et al. 2011). Among 3700 SCUSS fields, 3070 are fully covered by the SDSS and the total sky coverage is 3415 deg^2.

To ensure the uniformity of the photometry of the final sample of galaxies, we make further detailed selections on both the SCUSS and SDSS data.

Bright star mask. Bright stars contaminate the photometry of both the SCUSS and SDSS data. We use the bright star masks of the BOSS tilling geometry[7] to remove the area contaminated by these stars (Blanton et al. 2003). For a 3415 deg^2 SCUSS/SDSS area, the total area inside the bright star masks amounts to 33.88 deg^2.

SCUSS exposure time selection. In each field of the SCUSS, even for the combined image, not all areas have been covered by two exposures because of the gaps in the CCD camera (Zou et al. 2015). Figure 1 shows an example of the exposure map for a typical SCUSS field. As can be seen, there are a few stripes at the CCD gap regions with only one exposure, whereas a few overlapped regions have more than two exposures. To ensure a uniform optical depth in the galaxy number counts, we take the survey exposure map and only select galaxies inside the field with more than one exposure. With such a selection, the sky coverage of the SCUSS/SDSS data is further reduced to 2987 deg^2.

SDSS poor photometry. In the SDSS, there are image masks indicating poor photometry.[8] Inside the SDSS/SCUSS

[7] http://www.sdss3.org/dr9/algorithms/boss_tiling.php

[8] http://data.sdss3.org/sas/dr9/boss/lss/badfield_mask_unphot-ugriz_pix.ply

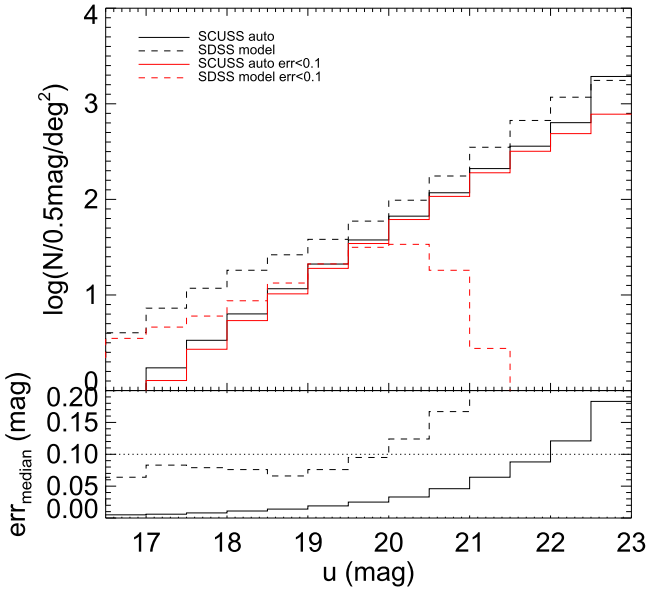

Figure 2. Number counts and photometric errors of galaxies in the SCUSS and SDSS. Top panel: the black solid and dashed histograms show the number counts of galaxies in the SCUSS and SDSS respectively, while the red solid and dashed histograms further show the galaxies with photometric error < 0.1. Bottom panel: the median of photometric errors of the SCUSS (solid) and SDSS (dashed) galaxies. A horizontal line $err_{median} = 0.1$ is shown for illustration.

overlapping area (2987 deg^2 after removing the SCUSS gaps), the total area with poor photometry masks adds up to 18.17 deg^2. For the SCUSS, the photometry of all fields is good since all poor fields have been observed repeatedly.

In summary, when we do the galaxy number counts in the SCUSS, we only select galaxies in an area with at least two exposures and avoid areas contaminated by bright stars. When we include the SDSS photometry to study the $u - r$ colors in Section 4, we further exclude the galaxies within the SDSS poor photometry mask. We take the "automatic magnitude" for galaxy number counts and use the "model magnitude" when studying their $u - r$ colors.

2.3. Galaxy Number Counts in SCUSS

In Figure 2, the top panel shows the histogram of the galaxy number counts in the SCUSS u band whereas the bottom panel shows the median photometric error in each given magnitude bin (solid histograms). We also plot the SDSS u-band results as the dashed histograms for comparison.

Apparently, the number counts of galaxies in the SDSS u band outnumbers the SCUSS data (top panel). The main reason for this outnumbering is that the "modelMag" in the u band of the SDSS is a forced measurement based on the profile model of the SDSS r band which is even deeper than the SCUSS u-band data for typical galaxies (see $u - r$ color distribution of galaxies in Section 4). Because of this, the SDSS u-band data have significantly larger photometric errors than the SCUSS sources (bottom panel). To further illustrate this, we also show the number counts of the SDSS and SCUSS u-band galaxies with photometric error smaller than 0.1 mag as the red dashed and red solid histograms in the top panel. After removing the objects with high photometric uncertainty, the SDSS u-band number counts match the SCUSS data at the bright end

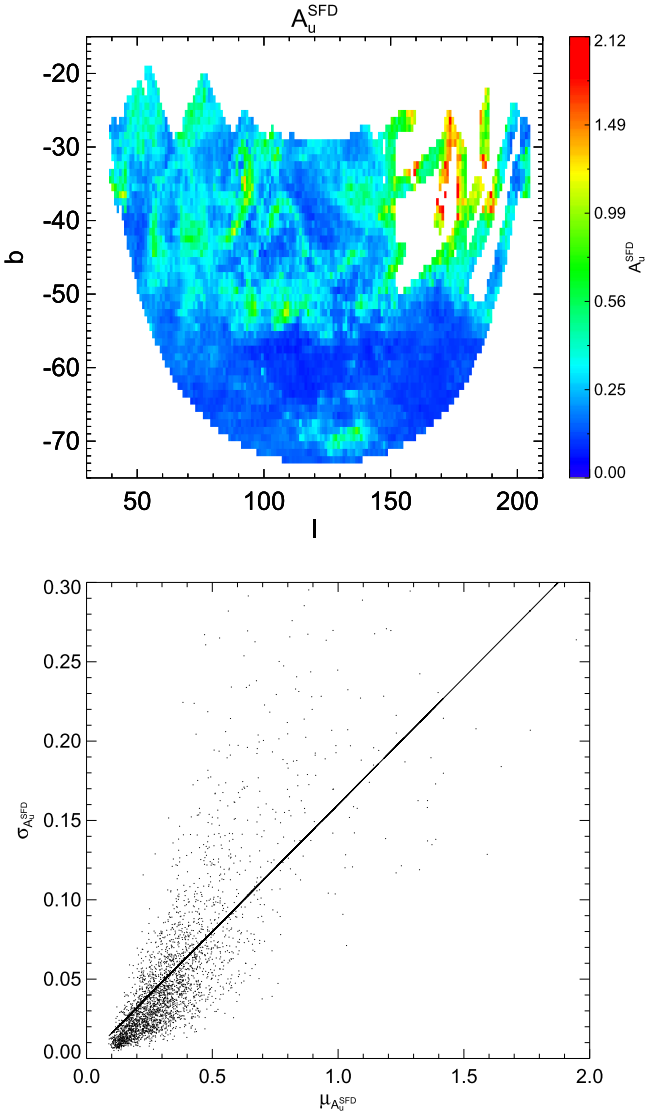

Figure 3. The u-band SFD extinction (A_u^{SFD}) map of 3070 SCUSS fields (top panel). The mean($\mu_{A_u^{SFD}}$) and scatter($\sigma_{A_u^{SFD}}$) of the A_u^{SFD} distribution of all SCUSS fields are shown in the bottom panel, where the solid line shows the relation $\sigma_{A_u^{SFD}} = 0.16\mu_{A_u^{SFD}}$.

($u < 20$) more closely. However, the galaxies in the SDSS u band still outnumber the SCUSS catalog at the very bright end ($r < 18$ mag). To further verify these excess detections in the SDSS, we have made visual inspections of both SDSS and SCUSS u-band images. We find that, except for fake detections from diffraction spikes of bright stars, most of these "bright objects" are caused by the forced fitting of the model magnitude with unrealistically large apertures.

3. GALACTIC EXTINCTION IN THE u BAND

In this section, we take the SCUSS galaxy catalog and use their number counts to study the Galactic extinction and compare it with the SFD extinction map. The SFD extinction map in the u band (using the ODO extinction curve with $R_V = 3.1$) of the 3070 SCUSS/SDSS fields is shown in the top panel of Figure 3 (in Galactic coordinates). As can be seen, because of the high extinction coefficient in the u band ($A_u^{SFD} = 5.108E(B - V)^{SFD}$), the expected A_u^{SFD} extinction values span a very wide range even for our high Galactic

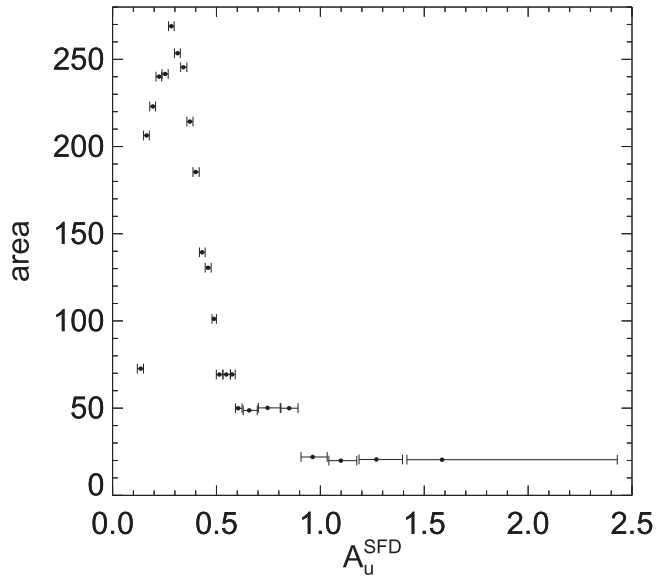

Figure 4. Area and mean A_u^{SFD} of the combined regions for galaxy number counts. The error bars show the ranges of the A_u^{SFD} of each combined region.

latitude footprint ($b < -20°$), from the lowest, ~0.11 mag, to as high as ~1.5 mag for a few regions.

The sky resolution of the SFD maps is 6.′1 per pixel. Inside a pixel of the SFD extinction map, the number of galaxies is too small for a statistical study. Even for a $1.^{\circ}08 \times 1.^{\circ}03$ SCUSS field, the number of galaxies is still not large enough to make high-accuracy statistics. Nevertheless, the aim of this study is not to obtain a high-resolution Galactic extinction map from galaxy number counts, but to make a systematic comparison of the Galactic extinction with the SFD map. Therefore, we gather as large as possible sky coverage with similar Galactic extinction to achieve high statistical significance.

Similar to the approach in Yasuda et al. (2007), we partition the total SCUSS/SDSS fields into 25 combined regions according to the A_u values of the SFD map. For simplicity, we take each SCUSS field as a unit to build the combined regions if the Galactic extinction inside it is close to a uniform distribution. To be specific, we calculate the mean and standard deviation of the A_u^{SFD} distribution for each SCUSS field (see the bottom panel of Figure 3). These SCUSS fields with normalized standard deviations smaller than 0.16 (the typical uncertainty of the SFD map) are then considered to have uniform A_u distributions. As can be seen from the bottom panel of Figure 3, the majority of the fields (2134 of 3070) are located below the separation line ($\sigma_{A_u^{SFD}} = 0.16\,\mu_{A_u}^{SFD}$), i.e., satisfying the uniform criteria. For the remaining 936 patchy fields, we further divide each of them into 6×6 sub-fields ($10.'8 \times 10.'3$). After that, the Galactic extinction distributions inside all these sub-fields satisfy the uniform criteria again. Combining all these uniform fields and sub-fields, we finally obtain 35,830 "units." We then rank these units according to their mean A_u values. There are 72 "units" with very low extinction ($A_u^{SFD} < 0.12$), which are combined as our reference region (see further details below). Next, for the "units" with $0.12 < A_u^{SFD} < 0.48$, we set the bin width of A_u^{SFD} to 0.03 mag and get 12 bins. For high extinction regions ($A_u^{SFD} > 0.48$), we require each combined region to have at least 20 deg^2 sky coverage so as to ensure statistical significance. With this requirement, we obtain a further 12 combined regions within the range $0.48 < A_u^{SFD} < 2.43$. In Figure 4, we show the total areas of all combined regions as a function of their A_u^{SFD} ranges.

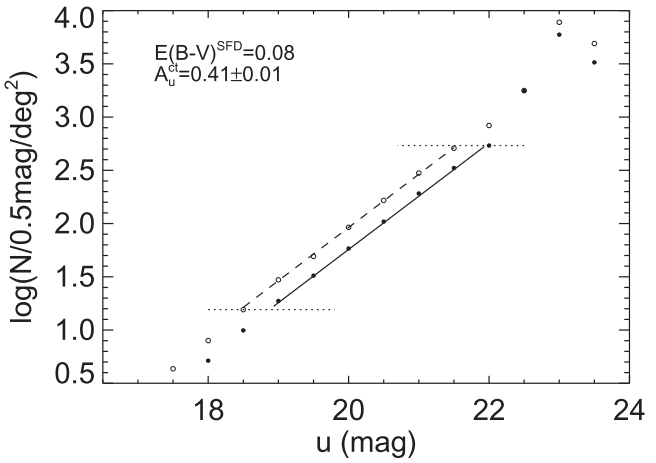

Figure 5. The SCUSS u-band galaxy number counts in the reference region (open circles) and the example region ($0.39 < A_u^{SFD} < 0.42$, filled circles). The dashed and solid lines are the fitting relations of Equations (1) and (2) respectively, whose fitting ranges are shown by the dotted lines.

We derive the Galactic extinction in the SCUSS u band by comparing the galaxy number counts of the extincted regions with that of the reference region (Fukugita et al. 2004; Yasuda et al. 2007). For the reference region, we correct the magnitudes of galaxies using the Galactic extinction values from the SFD map. We show the SCUSS u-band galaxy number count distributions (in terms of the number of galaxies per square degree per 0.5 mag) of an example region and the reference region as the filled and open circles in Figure 5 respectively. The example region is taken from Figure 4 where $0.39 < A_u^{SFD} < 0.42$ ($E(B-V) \sim 0.08$).

For both the reference and extincted regions, the galaxy number counts in the magnitude range ($18 < u < 22$) show nice linear relations in the logarithm space. We fit a linear relation for the reference region with the equation

$$\log N = \alpha(u - 20) + \beta. \quad (1)$$

Then, we fix the α and β values and fit a relation

$$\log N = \alpha(u - \Delta M - 20) + \beta \quad (2)$$

for the extincted region. Obviously, the fitting parameter ΔM is the average Galactic extinction of the extincted region.

It is worth mentioning that, to have self-consistent fitting results, the fitting range of the extincted region should also be shifted from the reference region by an amount ΔM. More specifically, we set the fitting ranges to be $18.5 < u < 22.0 - \Delta M$ and $18.5 + \Delta M < u < 22.0$ for the reference and extincted region respectively. The upper magnitude limit $u < 22$ mag is chosen where the SCUSS photometric error is smaller than 0.1 mag (Figure 2), whereas the lower magnitude is selected where the Poisson error of the galaxy number counts is smaller than 5%. The fitting result (ΔM) and fitting ranges are finally obtained by iteration. We show the results of the two fitting relations as the dashed line (reference region) and solid line (extincted region) in Figure 5. For this example region, the Galactic extinction A_u^{ct} we obtain is $\Delta M = 0.41 \pm 0.01$, which is in excellent agreement with the SFD map values ($A_u^{SFD} = 0.41$). The error of ΔM is estimated from the bootstrap sampling of the SCUSS galaxies.

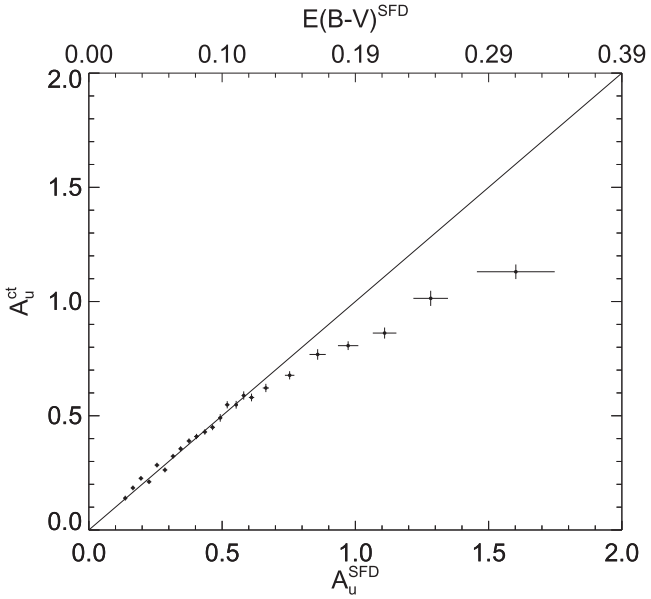

Figure 6. Mean and uncertainty of the Galactic extinction $A_u^{\rm ct}$ from galaxy number counts of all 24 regions, plotted against $A_u^{\rm SFD}$, the average extinction values from the SFD map. The horizontal error bars are the standard deviations of the $A_u^{\rm SFD}$ distributions in each region.

We undertake galaxy number count studies for all 24 combined regions and then compare the resulted $A_u^{\rm ct}$ estimations with the SFD values in Figure 6. As can be seen, for low extinction regions ($A_u^{\rm SFD} < 0.6$ mag), the extinction values derived from galaxy number counts are in excellent agreement with the SFD values. However, for high extinction regions ($A_u^{\rm SFD} > 0.6$ mag), the SFD values are systematically higher.

As we have mentioned, $A_u^{\rm SFD}$ is derived from $E(B-V)^{\rm SFD}$, whereas $E(B-V)^{\rm SFD}$ is converted from the 100 μm infrared flux. Both conversions use the standard $R_V = 3.1$ ODO extinction curve (see the Appendix for details). Therefore, the overestimation of $A_u^{\rm SFD}$ at high extinction regions either comes from the overestimation of the Galactic dust (conversion from the 100 μm flux) or a systematical variation of the extinction curve, or both. We leave the discussion of the variation of the extinction curve to Section 5. Assuming the Galactic extinction curve does not show systematic change at high extinction regions, our results indicate that the SFD map has overestimated the Galactic extinction by up to 40% for the $E(B-V) > 0.2$ mag regions.

4. GALACTIC REDDENING IN $u-r$

In this section, we further use the $u-r$ color distribution of galaxies to test the Galactic reddening of the SFD map. For SCUSS galaxies with $u < 23$, except the extreme blue ones ($u-r < 0.8$, not used in our statistical study), the $u-r$ color of all other galaxies can be matched from the SDSS r-band photometry catalog (complete to $r < 22.2$).

To measure the Galactic reddening of galaxies, a statistical quantity, i.e., the intrinsic color of galaxies, need to be well defined. Strateva et al. (2001) studied the $u-r$ colors of SDSS galaxies and found that galaxies can be separated into two populations with the separation at $u-r = 2.22$. In this study, we use the $u-r$ color peak of the blue galaxies ($u-r < 2.22$) as a statistical measurement. Unlike the mean or median of the galaxy colors, the peak of the $u-r$ distribution has the advantage of being unbiased by the incompleteness of the galaxies with extreme colors (e.g., the $u-r < 0.8$ galaxies in our study). Using the algorithm in Section 3, we partition the SDSS/SCUSS footprint into 25 regions according to their SFD $E(B-V)$ values. For each region, we select the galaxies with $u < 23$ and measure the peak of their $u-r$ distribution. More specifically, we assume that the $u-r$ color of each individual galaxy follows a Gaussian probability distribution function,

$$P_i(x) = \frac{1}{\sqrt{2\pi}\sigma_i}\exp\left(\frac{-(x-\mu_i)^2}{2\sigma_i^2}\right) \quad (3)$$

where μ_i and σ_i are its observed $u-r$ color and photometric uncertainty. The global $u-r$ distribution of the sampled galaxies is then obtained by adding the $u-r$ probability distributions of individual galaxies

$$P(u-r) = \frac{1}{N}\sum_{i=1}^{N} P_i(u-r), \quad (4)$$

where N is the number of galaxies ubnder consideration. We measure the peak of the resulting $u-r$ distribution in steps of 0.01 mag and estimate its uncertainty after 50 iterations of bootstrap samplings.

We show the $P(u-r)$ distributions of the galaxies in the reference region and the example region ($0.39 < A_u^{\rm SFD} < 0.42$) as solid and dotted curves in Figure 7 respectively. As expected, the peak of $P(u-r)$ in the example region shows a significant shift to the reference region, which tells us how much the galaxy colors are averagely reddened in the reference region. However, this shift is not the exact average Galactic reddening value we want to derive.

Galaxies have an intrinsic color–magnitude relation, i.e., brighter galaxies also appear redder. The Galactic dust not only reddens the galaxy's color but also extincts its flux. Therefore the galaxies with $u < 23$ mag in the extincted region are intrinsically brighter than the $u < 23$ mag galaxies in the reference region, which makes the galaxies in former region intrinsically bluer. To quantify this intrinsic color–magnitude relation, we separate the galaxies into different u-magnitude

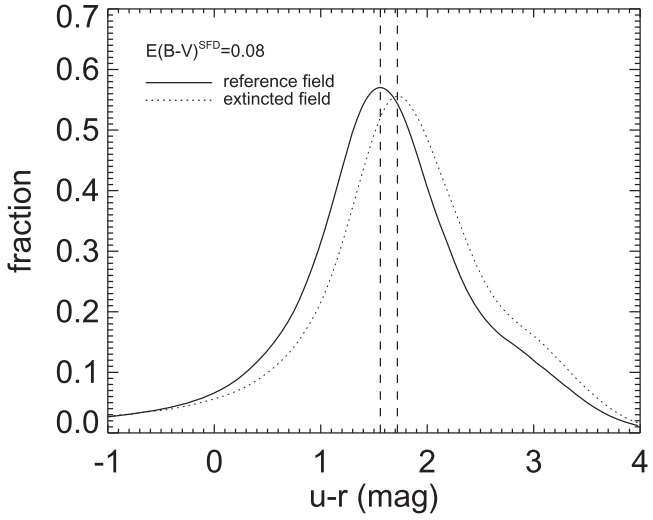

Figure 7. The $u-r$ distribution of galaxies. The solid and dotted curves show the results of the reference region and the example region ($E(B-V)^{\rm SFD} = 0.08$) respectively. The two dashed lines show the positions of the peaks of the two distributions.

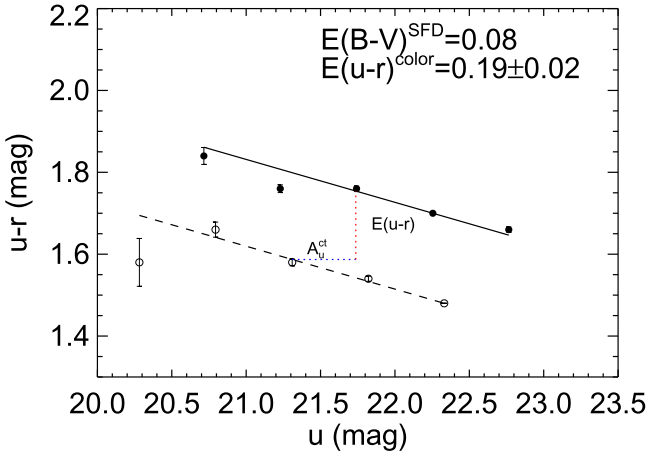

Figure 8. Color–magnitude relation and Galactic reddening of the example region ($0.39 < A_u^{\rm SFD} < 0.42$). The open and filled circles show the $(u-r)$–u relations of the reference region and example region respectively, whereas the dashed and solid line show the fitting relations of Equations (5) and (6).

bins and measure the peak of their $u-r$ colors accordingly. As an example, we plot the peak of the $u-r$ distribution as function of u magnitude in Figure 8 for the example and reference regions. Color–magnitude relations are clearly seen for both samples. We fit a linear relation between the $u-r$ peak color and u magnitude for the reference region

$$u - r = \alpha'(u - 21.5) + \beta' \tag{5}$$

and then fit the corresponding relation

$$u - r + E(u - r) = \alpha'(u - A_u - 21.5) + \beta' \tag{6}$$

for the extincted region, where α' and β' are fixed to the fitting values of Equation (5). In Equation (6), $E(u-r)$ and A_u are the average reddening and extinction of the given extincted region respectively. For each extincted region, the average extinction A_u has already been obtained from the galaxy number counts in Section 3 (Figure 6). For consistency, we set the fitting ranges of Equations (5) and (6) to be $20.0 < u < 23 - A_u$ mag and $20.0 + A_u < u < 23$ mag respectively. The fitting ranges of Equations (5) and (6) are fainter than those of Equations (1) and (2), which is due to the fact that we need more galaxies to constrain the $u-r$ color peak. The average Galactic reddening of the example region obtained from Equation (6) is $E(u-r) = 0.19 \pm 0.02$, which is also in excellent agreement with the SFD value $E(B-V) = 0.08$ for the standard $R_V = 3.1$ ODO extinction curve.

The average Galactic reddening $E(u-r)$ of all 24 regions is shown in Figure 9. In this plot, the $E(u-r)$ from the color distribution is plotted against the mean $E(u-r)$ from the SFD map, which is converted from $E(B-V)^{\rm SFD}$ using the standard $R_V = 3.1$ ODO extinction curve. We see that the $E(u-r)$ values from galaxy colors are highly consistent with the SFD results at the low reddening regions ($E(B-V)^{\rm SFD} < 0.12$). Again, for the high reddening regions ($E(B-V)^{\rm SFD} > 0.12$), the SFD reddening values deviate from the galaxy color measurements systematically. These results are very close to the galaxy number count results shown in Figure 6.

To have a better combination of the results from Figure 6 and Figure 9, we plot the differences of the $E(B-V)$ values between our measurements and the SFD map as function of $E(B-V)^{\rm SFD}$ in Figure 10. The $A_u^{\rm ct}$ and $E(u-r)^{\rm color}$ are both

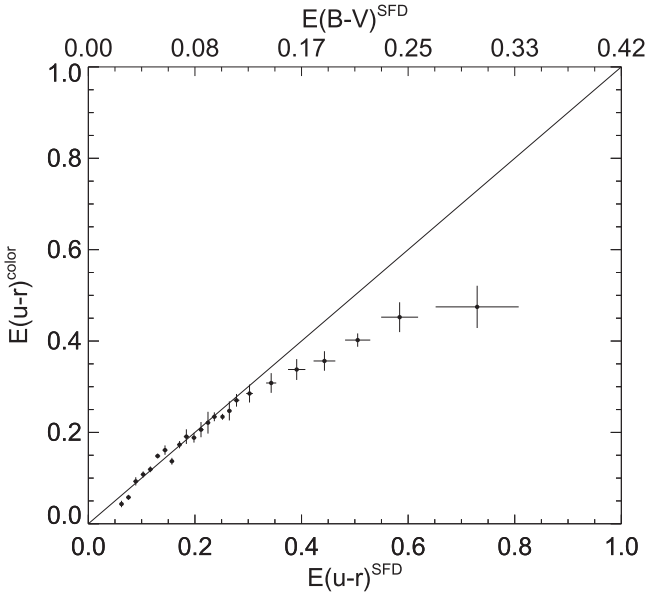

Figure 9. The Galactic reddening $E(u-r)^{\rm color}$ from color distributions of galaxies in all 24 regions, plotted against the mean $E(u-r)^{\rm SFD}$ from the SFD map.

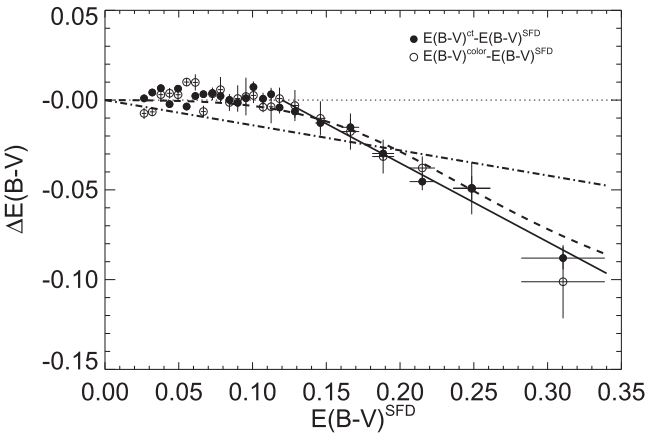

Figure 10. Differences of the $E(B-V)$ values between our measurements and the SFD map as a function of $E(B-V)^{\rm SFD}$. The open and filled circles show the results from $u-r$ galaxy colors and u band galaxy number counts respectively. The dotted, dashed, dotted–dashed, and solid lines are the $\triangle E(B-V) = 0$, Yasuda et al. (2007) results, $\triangle E(B-V) = -0.14E(B-V)$ of Schlafly & Finkbeiner (2011), and the linear fitting relation of Equation (7).

converted back to $E(B-V)$ values using the ODO $R_V = 3.1$ extinction curve. The two methods show very consistent results, indicating that the SFD map overestimates the reddening values at high extinction regions systematically. Such an overestimation can be approximated by a linear relation

$$\Delta E(B - V) = 0.43[E(B - V)^{\rm SFD} - 0.12] \tag{7}$$

when $E(B-V)^{\rm SFD} > 0.12$, which is shown by the solid line in Figure 10. We also plot the fitting relation of Yasuda et al. (2007) (their Equation (2)) and the result of Schlafly & Finkbeiner (2011) ($E(B-V) = 0.86E(B-V)$) as the dashed and dotted–dashed lines respectively for comparison. Our result is in good agreement with that of Yasuda et al. (2007).

Both our study and that of Yasuda et al. (2007) use the galaxy number counts whereas the work of Schlafly & Finkbeiner

(2011) uses the blue tip of the stellar locus to constrain the Galactic reddening. Moreover, the footprint of our study and that of Yasuda et al. (2007) are both in the South Galactic Cap region (although our footprint is much larger), whereas the study of Schlafly & Finkbeiner (2011) is mainly in the north Galactic sky. Therefore, the different $\Delta E(B-V)$ correction of Schlafly & Finkbeiner (2011) may either come from the systematics of the method or from the different reddening properties in Galactic coordinates.

5. DISCUSSION: GALACTIC EXTINCTION CURVE

In Sections 3 and 4, all Galactic extinctions and reddenings from the SFD map are derived using the standard ODO $R_V = 3.1$ extinction curve. However, as shown in the Appendix, all these values are model (extinction curve) dependent. We question whether the inconsistent results with the SFD map seen at the high extinction regions could be reconciled by introducing extinction curves with other R_V values or other models of the extinction curve, under the assumption that the dust emission provide by the SFD is correct.

5.1. Extinction Curve with Different R_V Values

As we have shown in Figures 6 and 9, the Galactic extinction and reddening are systematically overestimated by the SFD map when using the standard $R_V = 3.1$ extinction curve. However, this overestimation may also be explained using an extinction curve with higher R_V values. Indeed, some studies have shown that R_V increases toward the dense star-forming regions (e.g., Savage & Mathis 1979; Cardelli et al. 1988; Wang et al. 2013).

To test this idea, we convert the $E(B-V)$ values from the SFD map back to the Galactic extinction at the near-infrared wavelength 1 μm ($A_{1\,\mu\mathrm{m}}$), which is believed to be no longer dependent on the Galactic extinction curve. We plot A_u^{ct} and $E(u-r)^{\mathrm{color}}$ against $A_{1\,\mu\mathrm{m}}$ in the top and middle panels of Figure 11 respectively. At given $A_{1\,\mu\mathrm{m}}$, A_u and $E(u-r)$ can be easily predicted for the extinction curves with different R_V values (see the Appendixfor details).

As expected, at low extinction regions (small $A_{1\,\mu\mathrm{m}}$), our results are in good agreement with the $R_V = 3.1$ extinction curve. At high extinction regions, it seems that the inconsistency between our results and the SFD values can be reconciled by using the extinction curves with higher R_V values. To further test this idea, we force the A_u^{ct} and $E(u-r)^{\mathrm{color}}$ values to be consistent with the $A_{1\,\mu\mathrm{m}}^{\mathrm{SFD}}$ values (the two solid lines in the top and middle panels of Figure 11) and calculate the required R_V values in turn, which are shown as the solid and dashed lines in the bottom panel of Figure 11. As can be seen, we cannot achieve self-consistent results between the galaxy number counts and color distribution by only varying the R_V values of the extinction curves.

5.2. ODO versus FM Extinction Curve

The A_u^{ct} and $E(u-r)^{\mathrm{color}}$ values, besides both being model (extinction curve) independent, also provide a strong constraint on the shape of the Galactic extinction curve when combined. In Figure 12, we plot A_u^{ct} against $E(u-r)^{\mathrm{color}}$ values and compare their relation with the results of the two most frequently used extinction curves, the ODO and Fitzpatrick (1999) (FM) curves. For the $R_V = 3.1$ ODO and FM extinction

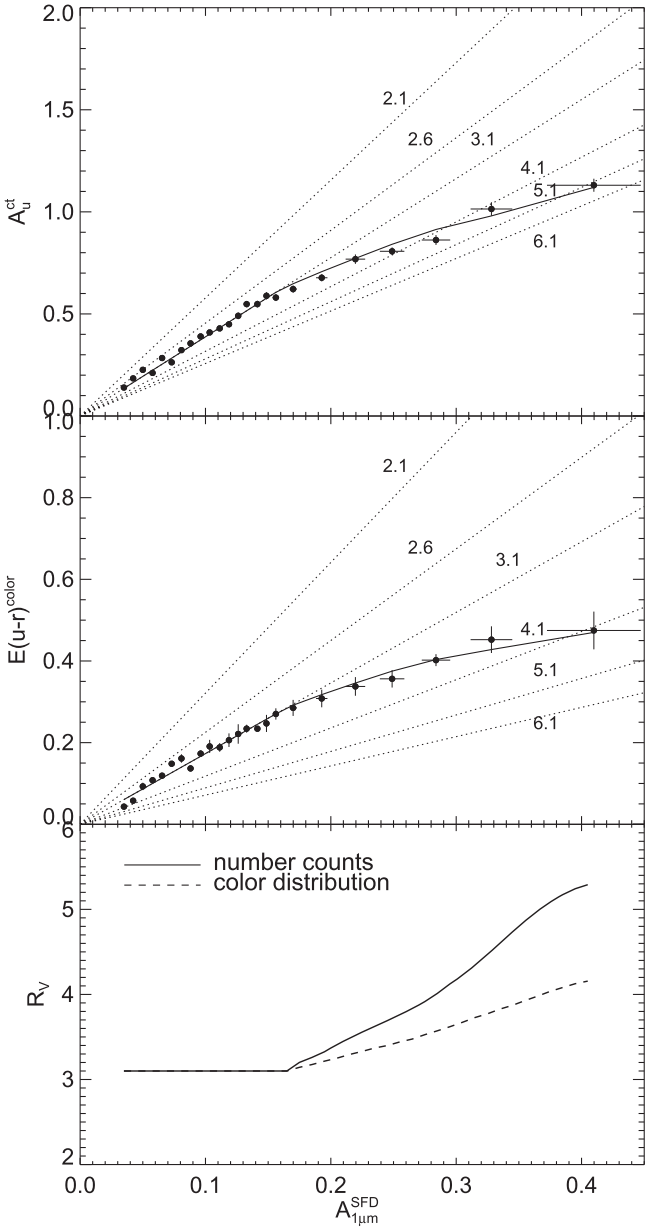

Figure 11. The Galactic extinction A_u^{ct} (top), reddening $E(u-r)^{\mathrm{color}}$ (middle), and the required R_V values (bottom) as a function of $A_{1\,\mu\mathrm{m}}^{\mathrm{SFD}}$. The dotted lines in the top two panels show the predicted A_u and $E(u-r)$ values as a function of $A_{1\,\mu\mathrm{m}}$ for ODO extinction curves with different R_V values. In the bottom panel, the solid and dashed lines show the required R_V values as a function of $A_{1\,\mu\mathrm{m}}$ when the predicted A_u and $E(u-r)$ values are forced to be consistent with the observational results (the solid lines in the top two panels respectively).

curves, the slopes of the A_u and $E(u-r)$ relation, i.e., the $A_u/E(u-r)$ values, are 2.203 and 2.114 respectively. As can be seen, the A_u^{ct} and $E(u-r)^{\mathrm{color}}$ relation is in excellent agreement with the ODO extinction curve, which is also significantly better than the FM one.

In order to further quantify the differences between the ODO and FM extinction curves, we impose a linear fitting on the relation of A_u^{ct} and $E(u-r)^{\mathrm{color}}$. Considering the uncertainty of the zero reddening of the reference region, we do not set the intercept of the fitting relation to be zero but as a free parameter. The fitting results we obtain are $A_u = (2.194 \pm 0.031)E(u-r) + (0.018 \pm 0.006)$. The intercept value from fitting is in agreement with zero, while the slope

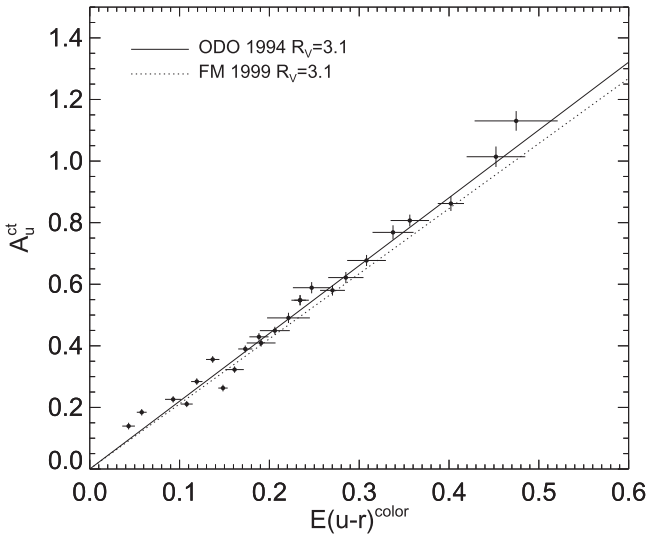

Figure 12. Correlation between the Galactic extinction $A_u^{\rm ct}$ from galaxy number counts and reddening $E(u-r)^{\rm color}$ from the color distribution. The solid and dotted lines show the relations between A_u and $E(u-r)$ from $R_V = 3.1$ ODO and FM extinction curves respectively.

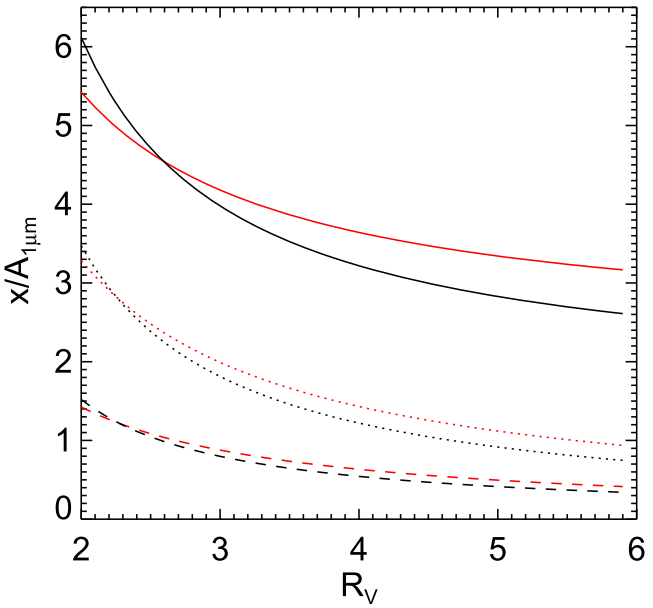

Figure 13. Extinction coefficient normalized to $A_{1\ \mu{\rm m}}$ as a function of R_V. The black solid, dotted, and dashed lines show $A_u/A_{1\ \mu{\rm m}}$, $E(u-r)/A_{1\ \mu{\rm m}}$, and $E(B-V)/A_{1\ \mu{\rm m}}$ using the ODO extinction law, while the results from the FM extinction law are shown in red.

value confirms that the ODO extinction curve is better than that of FM at about the 2.5σ level.

The excellent agreement with the ODO extinction curve of the A_u and $E(u-r)$ relation strongly implies that the overestimation of the Galactic reddening of the SFD values at high extinction regions is indeed caused by the overestimation of the infrared flux (or its conversion factor) and is unlikely be explained by the variation of the extinction curve.

6. SUMMARY AND CONCLUSION

In this paper, we use the galaxy catalog of South Galactic Cap *u*-band Survey to study the integral Galactic extinction and reddening using galaxy number counts and color distribution respectively. Benefiting from the sensitivity of the *u* band to dust extinction and SCUSS depth (1.5 mag deeper than the SDSS), we have obtained the average Galactic extinction $A_u^{\rm ct}$ and reddening $E(u-r)^{\rm color}$ in the South Galactic Cap region with unprecedented statistical accuracy. By combining the $A_u^{\rm ct}$ and $E(u-r)^{\rm color}$ results, we constrain the shape of the Galactic extinction curve and find that it is in excellent agreement with the standard $R_V = 3.1$ ODO extinction law. Our results also confirm that the SFD map overestimates the Galactic extinction at higher extinction regions ($E(B-V) > 0.12$). This overestimation is up to the level of about 40% and can be corrected using a linear relation $\Delta E(B-V) = 0.43[E(B-V)^{\rm SFD} - 0.12]$. As already discussed in Yasuda et al. (2007), this overestimation may be caused by the underestimation of the dust temperature of the 100 μm emission when constructing the SFD extinction map.

The footprint in this study is located in the high Galactic region where Galactic reddening does not reach a very high extinction value, such as that in the Galaxy disk. The maximum $E(B-V)$ value we can statistically probe is about 0.35. Therefore, the overestimation and correction of the SFD map we find at $E(B-V) > 0.12$ (Equation (7)) may only be valid in the range $0.12 < E(B-V) < 0.35$. Moreover, although our study covers a large footprint of the South Galactic Cap region (~3000 deg^2), we caution that this conclusion may also only be valid in the studied areas. As shown by Welty & Fowler (1992) and Fitzpatrick (1999), the Galactic extinction pattern (dust properties) may vary significantly at difference locations. Independent measurements of the Galactic extinction and reddening (as in our study) in very highly extincted regions and with all-sky coverage are worth further study.

L.L. thanks Hengxiao Guo and Shuai Feng for help of useful discussions. This work was supported by the National Natural Science Foundation of China (NSFC) with the Project Numbers 11573050, 11433003, 11433005, the "973 Program" 2014 CB845705 and the Strategic Priority Research Program "The Emergence of Cosmological Structures" of the Chinese Academy of Sciences (CAS; grant XDB09030200). Y.F.T. is supported by NSFC with No.11303070.

APPENDIX
GALACTIC EXTINCTION AND REDDENING FROM THE SFD MAP

In SFD, the 100 μm thermal emission is converted to reddening $E(B-V)$ by $E(B-V) = pD^T$, where p is a calibration coefficient, and D^T represents the point source-subtracted *IRAS*-resolution 100 μm emission corrected by a temperature factor. In the released SFD map of $E(B-V)$, p is calculated using the standard $R_V = 3.1$ ODO extinction law and then calibrated using the colors of elliptical galaxies.

For extinction curves other than the standard ODO $R_V = 3.1$ one, the released SFD $E(B-V)$ map cannot be directly used to calculate the Galactic extinction and reddening values. Alternatively, the $E(B-V)$ values of the SFD map can be converted back to the Galactic extinction at a near-infrared wavelength (e.g., 1 μm), which is believed to be very weakly dependent on the extinction curve. Then, the Galactic extinction curves can be expressed as

$$k(\lambda) = A(\lambda)/A(1\ \mu{\rm m}). \quad (8)$$

For a given $A_{1\,\mu m}$ value, the Galactic extinction in any given band b is calculated by

$$A_b = -2.5 \log \left[\frac{\int d\lambda W_b(\lambda) S(\lambda) 10^{-k(\lambda) A_{1\,\mu m}/2.5}}{\int d\lambda W_b(\lambda) S(\lambda)} \right] \quad (9)$$

where $W(\lambda)$ is the transmission curve of the given band, and $S(\lambda)$ is the source spectrum. The transmission curve is a convolution of the filter transmission, CCD quantum efficiency, and atmospheric extinction, which are publicly available for all photometric bands.[9] For $S(\lambda)$, we take the mean galaxy spectrum from the SDSS. We have tested that a more realistic source spectrum makes negligible changes to all of our results.

For a given extinction curve, we calculate the extinction coefficient $k(b) = A_b/A_{1\,\mu m}$ for all the related bands. The resulting $A_u/A_{1\,\mu m}$, $E(u-r)/A_{1\,\mu m}$, and $E(B-V)/A_{1\,\mu m}$ values are plotted as function of R_V values for FM and ODO extinction curves in Figure 13.

REFERENCES

Aihara, H., Allende Prieto, C., An, D., et al. 2011, ApJS, 193, 29
Arce, H. G., & Goodman, A. A. 1999, ApJL, 512, L135
Bertin, E., & Arnouts, S. 1996, A&AS, 117, 393
Blanton, M. R., Lin, H., Lupton, R. H., et al. 2003, AJ, 125, 2276
Burstein, D., & Heiles, C. 1982, AJ, 87, 1165
Cardelli, J. A., Clayton, G. C., & Mathis, J. S. 1988, ApJL, 329, L33
Cardelli, J. A., Clayton, G. C., & Mathis, J. S. 1989, ApJ, 345, 245
Denney, K. D., Peterson, B. M., Pogge, R. W., et al. 2010, ApJ, 721, 715
Dobashi, K., Uehara, H., Kandori, R., et al. 2005, PASJ, 57, S1
Draine, B. T. 2003, ARA&A, 41, 241
Fitzpatrick, E. L. 1999, PASP, 111, 63
Fukugita, M., Yasuda, N., Brinkmann, J., et al. 2004, AJ, 127, 3155
González, R. A., Fruchter, A. S., & Dirsch, B. 1999, ApJ, 515, 69
O'Donnell, J. E. 1994, ApJ, 422, 158
Oguri, M. 2014, MNRAS, 444, 147
Peek, J. E. G., & Graves, G. J. 2010, ApJ, 719, 415
Savage, B. D., & Mathis, J. S. 1979, ARA&A, 17, 73
Schlafly, E. F., & Finkbeiner, D. P. 2011, ApJ, 737, 103
Schlafly, E. F., Finkbeiner, D. P., Schlegel, D. J., et al. 2010, ApJ, 725, 1175
Schlegel, D. J., Finkbeiner, D. P., & Davis, M. 1998, ApJ, 500, 525
Schröder, A. C., Mamon, G. A., Kraan-Korteweg, R. C., & Woudt, P. A. 2007, A&A, 466, 481
Strateva, I., Ivezić, Ž., Knapp, G. R., et al. 2001, AJ, 122, 1861
Wang, S., Gao, J., Jiang, B. W., Li, A., & Chen, Y. 2013, ApJ, 773, 30
Welty, D. E., & Fowler, J. R. 1992, ApJ, 393, 193
Yasuda, N., Fukugita, M., & Schneider, D. P. 2007, AJ, 134, 698
York, D. G., Adelman, J., Anderson, J. E., Jr., et al. 2000, AJ, 120, 1579
Yuan, H. B., Liu, X. W., & Xiang, M. S. 2013, MNRAS, 430, 2188
Zhou, X., Fan, X.-H., Fan, Z., et al. 2016, RAA, 16, 017
Zou, H., Jiang, Z., Zhou, X., et al. 2015, AJ, 150, 104
Zou, H., Zhou, X., Jiang, Z., et al. 2016, AJ, 151, 37

[9] The SCUSS u-band transmissions are available at http://batc.bao.ac.cn/BASS/doku.php?id=scuss:facilities:homefilter. The SDSS r-band data are avaliable at https://www.sdss3.org/instruments/camera.php.